

1



19

## Abstract

20 Watershed streamflow is often the focus of hydrological model calibration and evaluation,  
21 despite other potential objectives, including water quality management, flood protection, and  
22 agricultural management. When hydrological models are calibrated on streamflow,  
23 intermediate processes such as those affecting soil moisture are not necessarily well  
24 represented. This research evaluated the performance of downscaled and bias corrected soil  
25 moisture calibrated models against streamflow calibrated models both under single and multi-  
26 objective scenarios on field scale soil moisture estimation performance. Downscaled satellite  
27 soil moisture data and streamflow data are used to calibrate a Soil and Water Assessment Tool  
28 – Variable Source Area model initialized using topographic index classes to create hydrologic  
29 response units. In-situ soil moisture measurements at 25 locations across a 4-ha mixed-grass  
30 pasture located in southwestern Virginia were used to estimate field scale average soil moisture  
31 variability for model evaluation. Leveraging downscaled satellite soil moisture data  
32 substantially improved estimation of temporal soil moisture variability without affecting the  
33 model performance in estimating streamflow. The multi-objective calibration using streamflow  
34 and satellite soil moisture improved overall model performance both in estimating streamflow  
35 and soil moisture. A three-class topographic index hydrologic response unit definition allowed  
36 for adequate representation of saturation excess runoff process. Downscaling enabled  
37 calibration in a small 14 km<sup>2</sup> watershed using coarse satellite soil moisture data.

## 38 1 INTRODUCTION

39 Many parameters used in process-based hydrological models are difficult to determine or  
40 measure. Hence, parameter estimation and model calibration are used to ensure that a model



41 suitably represents a hydrologic system (Pechlivanidis et al., 2011). Watershed streamflow  
42 response is often the focus of hydrological model calibration and evaluation, despite many  
43 other potential objectives including water quality management, flood protection, agricultural  
44 management. Streamflow data is often used to calibrate a model because it is relatively easy to  
45 acquire and is a good integrator of the hydrological mass balance, as well as various processes  
46 occurring in the watershed, such as runoff generation, soil moisture redistribution, and  
47 evapotranspiration. However, calibrating a model on streamflow, when other processes are  
48 (also) of interest, may inadequately represent these other processes.

49 Calibrating models on hydrologic processes, such as soil moisture, requires sufficient  
50 information on these variables. However, at a watershed scale, direct and accurate soil moisture  
51 observation is time consuming and expensive (Vereecken et al., 2015). While methods exist to  
52 facilitate direct measurement of soil moisture, including time domain reflectometry (TDR),  
53 frequency domain reflectometry, and physical methods, such as the traditional gravimetric  
54 sampling, using these or similar point measurement techniques to monitor soil moisture  
55 variability in heterogenous watersheds requires an extensive network of measurement points  
56 (Brocca et al., 2010).

57 Distributed and continuous remotely sensed soil moisture data are becoming increasingly  
58 available, opening new avenues for incorporating and estimating soil moisture variability in  
59 hydrologic modelling (Brocca et al., 2017). Satellites dedicated to estimating the average  
60 surface moisture condition at several km resolution have become more common. The European  
61 Space Agency (ESA) Soil Moisture and Ocean Salinity (SMOS), the first mission dedicated to  
62 soil moisture (Mascaro et al., 2011, <https://earth.esa.int/eogateway/missions/smos>), is one  
63 example. The European Space Agency Climate Change Initiative soil moisture product has



64 daily temporal and  $0.25^0$  (~25 km) spatial resolutions (Han et al., 2020; Kundu et al., 2017).  
65 The NASA Soil Moisture Active Passive (SMAP) satellite mission is another example  
66 designed to collect surface soil moisture at 36 km spatial resolution at a daily temporal  
67 resolution (O'Neill et al., 2018). The Advanced Scatterometer (ASCAT) (H SAF, 2021) and  
68 Advanced Microwave Scanning Radiometer 2 (AMSR2) (Cho et al., 2015) are additional  
69 examples that provide soil moisture products, ranging in resolution from 10-25 km.

70 Previous studies have attempted to improve hydrological model performance by incorporating  
71 satellite soil moisture data into hydrological modelling frameworks. For instance, Nanda et al.,  
72 (2023) used Enhanced SMAP L3 9 km resolution product (SPL3SMP\_E) to calibrate the  
73 Variable Infiltration Capacity model reporting significant improvement in streamflow and  
74 drought estimation. Rajib et al., (2016) using AMSR ~1 cm soil moisture to calibrate a Soil  
75 and Water Assessment Tool (SWAT) model reported improved surface soil moisture  
76 estimation (~1cm) with no improvement in streamflow estimation and on soil moisture for  
77 deeper soil layers, which they attributed to SWAT's structural deficiency in its  
78 evapotranspiration mechanism. They showed soil moisture estimates for deep layers improved  
79 when in-situ observed (0-600mm) data from a single sensor is used together with streamflow  
80 to calibrate SWAT at the hydrologic response unit (HRU) level. However, their overall  
81 reported goodness of fit values for soil moisture remained low (Kling Gupta Efficiency = 0.14  
82 - 0.35,  $R^2 = 0.11 - 0.25$ ) for all scenarios tested. This overall poor performance can also be due  
83 to the direct use of point scale measurement of soil moisture as a representative estimate for  
84 HRU scale average soil moisture conditions. López López et al. (2017) showed that using  
85 several products (evapotranspiration, soil moisture, and streamflow) together to calibrate  
86 SWAT resulted in improved streamflow predictions than using soil moisture alone when



87 compared to estimates from a streamflow-calibrated model. In contrast, Dangol et al. (2023)  
88 calibrated SWAT using satellite soil moisture alone and improved soil moisture performance  
89 but reduced streamflow estimation performance. In addition, multi-objective calibration  
90 showed no improvement compared to calibration solely on streamflow. Reported  
91 improvements in soil moisture performance were not evaluated against in-situ soil moisture  
92 measurements, which is important given the uncertainty surrounding satellite soil moisture  
93 products. Others incorporated satellite soil moisture data using data assimilation techniques for  
94 updating model state instead of direct adjustment of model parameter values (Azimi et al.,  
95 2020; De Santis et al., 2021; Patil & Ramsankaran, 2017; Sun, 2016; Wakigari & Leconte,  
96 2023) and reported improved model simulation performance for streamflow. Fewer studies  
97 report the effect of incorporating satellite soil moisture products for model calibration on both  
98 soil moisture and streamflow estimation performance (Dangol et al., 2023; Eini et al., 2023;  
99 Rajib et al., 2016). For instance, Rajib et al. (2016) compared model estimated soil moisture  
100 against in-situ observations for both streamflow only and multi-objective model calibration;  
101 however, they reported low fitness values likely due to the scale of comparison, point  
102 measurements up to  $\sim 2 \text{ km}^2$  average model estimate. And while there is agreement that  
103 remotely sensed soil moisture can be used to calibrate a watershed model for improved soil  
104 moisture estimation, the scale of soil moisture outputs is still coarse ( $> 2\text{km}^2$ ), and additional  
105 effort is required to inform field-scale management applications.

106 There are several challenges to incorporating remotely sensed satellite soil moisture products  
107 into hydrological model calibration. The resolution of satellite soil moisture products presents  
108 a challenge for use in small watersheds of size less than the soil moisture product resolution.  
109 Studies that use satellite soil moisture data for model calibration occur primarily in watersheds



110 larger than  $\sim 700 \text{ km}^2$  (Dangol et al., 2023; Eini et al., 2023; López López et al., 2017; Rajib  
111 et al., 2016). Downscaling satellite soil moisture data to capture finer resolution variabilities  
112 may extend the use of satellite soil moisture data for constraining watershed model parameters  
113 in watersheds  $< 100 \text{ km}^2$ .

114 In this work, a machine learning based downscaling technique is applied to generate high  
115 resolution (500 m) soil moisture data. In addition, while satellite soil moisture may represent  
116 average soil moisture condition at a watershed scale adequately, at a finer scale bias correction  
117 may be needed to ensure the range of soil moisture variability observed in in-situ measurements  
118 is suitably captured. The overall objective of this work was to evaluate the use of soil moisture  
119 data to calibrate a watershed model in a small saturation excess runoff dominated watershed.  
120 Specifically, to incorporate downscaled satellite soil moisture data into a high-resolution Soil  
121 and Water Assessment Tool (SWAT) - Variable Source Area (VSA) model (Easton et al.,  
122 2008) to improve soil moisture and streamflow estimates, and to quantify model parameter  
123 uncertainty under single and multi-objective calibrations. As illustrated in previous studies,  
124 SWAT-VSA can capture fine scale variabilities in runoff generation adequately by informing  
125 model structure using the topographic index (TI) in watersheds where saturation excess  
126 controls runoff generation (Beven et al., 2021). We compare the accuracy of soil moisture  
127 estimates from models calibrated against streamflow (SF), downscaled soil moisture (DSM),  
128 and a multi-objective (MO) streamflow/soil moisture model against in-situ soil moisture  
129 measurements at a fine spatial scale. An added benefit of the method is that it opens model  
130 application to areas without streamflow gaging stations.



## 131 2 MATERIAL AND METHODS

### 132 2.1 Soil Moisture Data

#### 133 2.1.1 SMAP Soil Moisture and Downscaling

134 The NASA Soil Moisture Active Passive (SMAP) is a global surface soil moisture acquisition  
135 mission (Entekhabi et al., 2014; O'Neill et al., 2023). The mission uses an L-band radiometer  
136 and L-band radar. The two instruments together meet the mission requirements of  $0.04 \text{ m}^3 \text{ m}^{-3}$   
137 accuracy at 9 km resolution (Entekhabi et al., 2014). However, the radar failed three months  
138 into the mission limiting data resolution to the radiometer sensor, currently 36 km. To  
139 overcome this gap in producing finer resolution products several methods have been applied.  
140 Interpolation techniques were used to generate a product at 9 km resolution (Chan et al., 2018);  
141 a data assimilation procedure and radar data from Sentinel-1 were used to generate a product  
142 at 3km resolution (Das et al., 2018); machine learning algorithms produced data at 1 km  
143 resolution (Abbaszadeh et al., 2021); and incorporating Kalman Filter into the Modified Palmer  
144 Two-Layer soil moisture model produced the National Aeronautics and Space Administration  
145 (NASA) and the United States Department of Agriculture (USDA) Enhanced SMAP at 10 km  
146 resolution.

147 The machine learning tool, 'mlhrsm' package in R (Peng et al., 2024) was used to further  
148 downscale the NASA-USDA Enhanced SMAP to 500 m resolution data for use in model  
149 calibration. The mlhrsm package in R uses a pretrained quantile random forest model for  
150 downscaling. The random forest model is trained using Sentinel-1 backscatter, MODIS land  
151 surface temperature, Landsat 8 (surface reflectance, NDVI and NDWI), United States  
152 Geological Survey (USGS) 10 m Digital Elevation Model (DEM), POLARIS (clay, sand and



153 bulk density), and NLCD land cover. The downscaling algorithm returns soil moisture data as  
 154 volumetric water content (VWC) for a target region at the selected 500 m resolution. The data  
 155 covers the period from April 2015 to August 2022.

#### 156 2.1.2 In-situ Soil Moisture

157 In-situ soil moisture was collected on 20 dates from 25 randomly selected points in a 4.2 ha  
 158 pasture in the 1-3 days following precipitation events for the period from March 2023 to  
 159 January 2024. Temporal variability of soil moisture was well represented in the data with  
 160 observations occurring on days near to the soil permanent wilting point and saturated soil  
 161 moisture conditions (0.15 – 0.45 volumetric water content). The daily average field scale soil  
 162 moisture was estimated from the 25-point measurements by using TI class distribution in the  
 163 field as an estimator for spatial moisture distribution. Calculated field scale average soil  
 164 moisture was used for model performance evaluation against model estimates across the same  
 165 domain, Fig. A1. Additional details on this dataset are reported in Asfaw et al., (2025).

#### 166 2.2 Study Area

167 Stroubles Creek is a 19.5 km long perennial stream draining a 57 km<sup>2</sup> watershed in the New  
 168 River Valley, VA, Fig. A2. In this study, the watershed outlet, 80° 26' 47'' W and 37° 12' 10''  
 169 N, is selected about 1 km downstream of the flow monitoring station where the stream drains  
 170 a 17.1 km<sup>2</sup> area. At this stream reach, the Stroubles Creek is a third order headwater stream  
 171 (Hofmeister et al., 2015) formed when two tributaries, the Central Branch and the Webb Branch  
 172 come together after draining the urban section of Blacksburg Town. Stroubles Creek watershed  
 173 is located in Montgomery County, Virginia. It is within the Valley and Ridge physiographic  
 174 region. Geologically the area is dominated by dolomite and limestone formations; springs and





175 sink holes are also present (Ketabchy, 2018; Parece et al., 2010). The area receives 1200 mm  
176 annual precipitation of which 760 mm is subject to evapotranspiration (Asfaw et al., 2025).  
177 The Virginia Tech StREAM Lab monitoring station, located at 80°26' 42'' W and 37°12' 37''  
178 N, is the stream flow data source; at this monitoring station the creek drains the upper 14.5 km<sup>2</sup>  
179 watershed. Most of the measurements have been active since 2012. A particular interest in this  
180 study is the stage/discharge data. The watershed has 67% pervious and 32% impervious land  
181 cover (Nayeb Yazdi et al., 2019).

## 182 2.3 SWAT-VSA model

183 SWAT is a semi distributed watershed scale hydrologic and water quality model. To simulate  
184 surface and subsurface runoff and various chemical and sediment export, SWAT requires  
185 landuse, soil, agricultural management, weather and topographic data. SWAT-VSA is a  
186 modification to SWAT to simulate variable source area hydrology VSA (Easton et al., 2008).  
187 To accomplish this, the curve number (CN) model of runoff generation is modified to  
188 continuously redistribute the average watershed soil moisture storage, S, based on terrain  
189 properties (Easton et al., 2008; Fuka et al., 2016). SWAT-VSA in addition to soil and land use  
190 uses TI values to build hydrologic response units (HRUs) (Easton et al., 2008).

191 SWAT computes the soil water content for each layer individually. Infiltration to the top layer  
192 is estimated after subtracting evaporative demand and surface runoff estimates from  
193 precipitation at a daily time step. SWAT directly handles saturated gravity flows in the vertical  
194 direction as percolation. Moisture depletion during unsaturated conditions is indirectly  
195 compensated through plant uptake and transpiration and soil water evaporation in the soil  
196 layers. These unsaturated moisture depletion mechanisms in the soil layers are often optimized



197 during model calibration by using the plant evapotranspiration compensation factor (EPCO)  
198 and soil evaporation compensation factor (ESCO) parameters.

199 SWAT assumes homogeneous moisture distribution in each soil layer. When the individual  
200 soil layer's depth in the model is very large, the uniform soil water distribution per soil layer  
201 assumption poses a problem by averaging moisture over large vertical depths. An adjustment  
202 is required before a direct comparison can be made between SWAT computed soil moisture,  
203 the downscaled surface soil moisture, and in-situ TDR measurements, where the latter two are  
204 for the top 50 mm and 120 mm soil depths, respectively. To ensure meaningful comparison,  
205 the SWAT output is modified to write out 0-50mm layer and a 50-120 mm layer in addition to  
206 standard layers in SWAT. Consequently, adding more layers can have an added benefit of  
207 accurately simulating moisture variability in the top layers during wetting and drying. In  
208 addition, since SWAT soil moisture output only reports the available water content in depth  
209 units, it is first converted to a volumetric basis and adjusted by the water content at a permanent  
210 wilting point for the dominant soil in the watershed.

### 211 2.3.1 Model Initialization

212 The SWAT model initialization was developed using ArcSWAT version 2012.10\_8.26 in  
213 ArcGIS Desktop 10.8.2. The 2019 landuse data were retrieved from the US Geologic Survey  
214 (USGS) National Land Cover Data (NLDC) website using the 'get\_nlcd' function from  
215 'FedData' package in R (Bocinsky et al., 2025; Jin et al., 2023). The USGS 3DEP program 1m  
216 resolution elevation data were used for watershed delineation, estimation of slope, and  
217 calculation of TI. The VSA initialization was executed using TopoSWAT (Fuka & Easton,  
218 2016) an ArcGIS plugin. The plugin was modified to enable three TI classes. Using Natural



219 Breaks from Spatial Analyst in Arc GIS, TI values were sliced into each class minimizing  
220 variance within class and maximizing variance among classes. The three TI classes from class  
221 3 to 1 cover 6%, 38%, and 56% of the watershed area, respectively. TopoSWAT downscales  
222 soil texture, soil depth, available water capacity, and hydraulic conductivity across TI classes.  
223 This was demonstrated to improve spatial representation of soil properties in VSA dominated  
224 watersheds (Fuka et al., 2016). Soils data were collected from the FAO-UNESCO Digital Soil  
225 Map (FAO, 2007). Weather data from the Global Historical Climatology Network (GHCN)  
226 were used for model forcing. The data were acquired using the 'FillMissWX' function in R  
227 (Garna et al., 2023).

## 228 2.4 Data for Model Calibration and Evaluation

### 229 2.4.1 Streamflow Data

230 The StREAM lab monitoring station collects stage readings at a frequency of 10-15 minutes.  
231 Model calibration and evaluation were performed at a daily timestep. To calculate daily  
232 average flow from the instantaneous stage records: first, stage was converted to flow using a  
233 rating curve developed for the location; second, a time series between the start and end dates  
234 was enumerated for each corresponding flow value including missing data using the zoo  
235 package in R (Zeileis et al., 2025); and third, mean daily flow values were calculated excluding  
236 dates with missing values for at least consecutive 12 hrs. The resulting data extended from  
237 2011 to 2024, a total of 14 years. The data for years 2011 and 2012 were excluded due to  
238 extended periods of missing values. The first 10 years period (Jan 2013 – Dec 2021) was used  
239 for model calibration and the last two years and five months (Jan 2022 - May 2024) period was  
240 used for model evaluation.



#### 241 2.4.2 Soil Moisture

242 The SWAT VSA model was initialized using the USGS 3DEP 1m resolution DEM, and areas  
243 of similar landuse, soil, and TI classes were intersected to form HRUs. Enhanced SMAP grid  
244 resolution is 100 km<sup>2</sup>, close to an order of magnitude larger than the watershed area (~14 km<sup>2</sup>).  
245 Therefore, the downscaled soil moisture data were averaged to the watershed scale and  
246 calibration at watershed level was assumed to be adequate. After initial downscaling, we  
247 compared the mean and range in the in-situ soil moisture data of the pasture against the  
248 downscaled satellite soil moisture data. This comparison revealed the downscaled satellite data  
249 had a narrower range and less variability than measured soil moisture, with the average satellite  
250 estimated maximum soil saturated moisture content of 32%, while the in situ saturated soil  
251 moisture reached 45%. To ensure comparable results, the downscaled soil moisture data was  
252 bias corrected for those days with significant precipitation input, Eq. (1). A three-day rolling  
253 mean was applied for smoothing after bias correction:

$$254 \quad \theta_{s,cor} = \begin{cases} \theta_s + k\sigma & \text{if } dP \geq d \\ \theta_s & \text{if } dP < d \end{cases} \quad (1)$$

255 Where  $\theta_{s,cor}$  is the bias corrected soil moisture,  $\sigma$  is average standard deviation of the  
256 uncertainty bound around the downscaled mean soil moisture estimates from the mlhrsm,  $\theta_s$   
257 is the average downscaled watershed soil moisture,  $k$  is a scaling factor, and  $d$  is a threshold  
258 effective precipitation depth in mm calculated as equivalent value to bring the top 120 mm soil  
259 from field capacity to saturation. The bias correction procedure resulted in satellite and in-situ  
260 soil moisture data with similar mean and range.

261 The downscaled, watershed average, and bias-corrected data were used for model calibration.

262 From here forward, these data are referred to simply as soil moisture data for brevity.



## 263 2.5 Model Calibration

### 264 2.5.1 Model Sensitivity

265 To identify the most influential parameters for calibration of a SWAT-VSA model a sensitivity  
266 analysis was performed. A total of 20 parameters to which streamflow predictions are sensitive  
267 and which have theoretical significance for soil moisture estimation were included in the  
268 sensitivity analysis. The analysis was executed using the relative sensitivity calculated based  
269 on successively evaluated Nash-Sutcliffe Efficiency (NSE) (Nash & Sutcliffe, 1970) values  
270 and corresponding value changes in parameters. The relative sensitivity values were calculated  
271 for model simulation from January 1, 2015, through December 31, 2019. Table 1 provides the  
272 tested parameters, and their rank based on relative sensitivity values.

### 273 2.5.2 Calibration Strategy

274 Calibration was performed by adjusting values of model parameters found to be influential on  
275 model outputs to maximize the agreement between observed and simulated values. The target  
276 model outputs were streamflow and average watershed soil moisture in the top 50 mm soil  
277 layer. Three model calibration approaches included calibration on streamflow, calibration on  
278 soil moisture data, and a multi-objective calibration on both streamflow and soil moisture data  
279 (multi-objective). Before the three separate calibrations were executed, parameters related to  
280 baseflow and snow processes were pre-calibrated following a stepwise calibration approach.  
281 The purpose of the baseflow and snow calibration was to find a suitable range for baseflow-  
282 related model parameters during the calibration. The snow parameters were set constant at pre-  
283 calibrated values because initial analysis indicated the values provide adequate estimation of  
284 snow fall component of the observed total precipitation. Baseflow separation was performed



285 using the 'baseflowseparation' function from EcoHydRology package (Fuka et al., 2013;  
286 Nathan & McMahon, 1990). Table 1 provides the calibrated parameters and their ranges for  
287 each method.

288 The two single-objective model calibrations were performed using a differential evolutionary  
289 algorithm, an exhaustive parameter space searching algorithm using mutations, crossover, and  
290 selection minimizing the model objective function defined on model efficiency measures. The  
291 algorithm was implemented using the 'DEoptim' R package (Mullen et al., 2011). The multi-  
292 objective calibration was performed using non-dominated sorting genetic algorithm (NSGAII),  
293 a multi-objective optimization algorithm using non-dominated sorting, crowding distance  
294 calculation, selection, crossover and mutation solving for the pareto front solution for the two  
295 objectives (Bekele & Nicklow, 2007; Deb et al., 2000). The NSGA-II algorithm identified a  
296 set of pareto solutions from which a solution is selected given the modeling objective. To select  
297 the best solution from the multi-objective pareto front solutions, in addition to maximizing the  
298 objective function on streamflow and satellite soil moisture data, the model accuracy in  
299 estimating the field scale soil moisture was evaluated using the in-situ soil moisture  
300 measurements. The algorithm was implemented using the Python library 'pymoo' (Blank &  
301 Deb, 2020).

302 To implement the CN based VSA implementation, a three TI class initialization was used. The  
303 TI classes divided the watershed into three zones, each with assumed uniform runoff generation  
304 and incrementally lesser propensity to generate runoff from TI class 3 (wet) to 1 (dry). These  
305 class identifications were incorporated into HRU delineation. The parameter CN2 (curve  
306 number for the average soil moisture conditions), was used to estimate the watershed average  
307 storage deficit S; and was updated after each calibration iteration in the management files



308 (\*.mgt) for each corresponding HRU. To distribute the value of average CN2 to class 1 (CN2-  
309 1), class 2 (CN2-2) and class 3 (CN2-3), as estimates of local storage deficit, the distribution  
310 relationship proposed in Easton et al. (2008) was used. Adjustment factors derived from this  
311 distribution were updated during each iteration based on the new estimate of the watershed  
312 average CN2. HRUs on low lying and converging landform were assigned to TI class 3 and  
313 the largest CN2 value corresponding to the smallest storage deficit, and consequently the  
314 greatest runoff. Initial estimates for CN2 were based on a simple water balance calculation  
315 using the method described in Lyon et al. (2004), while subsequent values were estimated by  
316 the optimization algorithm, but still maintaining the distribution of relative CN2 values.

### 317 2.5.3 Goodness of Fit Measures

318 Four complimentary goodness of fit measures, the coefficient of determination ( $R^2$ ), the root  
319 mean squared error (RMSE), the percent bias (PBIAS), and the Nash-Sutcliffe efficiency  
320 (NSE) were used to evaluate model performance (Krause et al., 2005; Moriasi et al., 2007).  
321 Calibration on streamflow was performed to maximize the NSE value as this is the most widely  
322 used approach. Compared to streamflow, soil moisture typically has smaller variances, but also  
323 a longer memory (i.e., soil moisture takes longer to recede than streamflow in humid climates).  
324 Soil moisture also has upper and lower bounds limited by the soil porosity and textural  
325 properties. The NSE normalizes the variance in observed data (Krause et al., 2005) and  
326 therefore may be overly sensitive to small errors in data with small variance. The RMSE is  
327 sensitive to the magnitude of error and can be a suitable objective function to reduce absolute  
328 error when estimating data with high frequency fluctuation. It is also a commonly used metric  
329 in satellite soil moisture validation studies (Entekhabi et al., 2010).



#### 330 2.5.4 Parameter Uncertainty

331 During calibration, DEoptim was set up to evaluate 13 parameter vectors in each iteration for  
 332 a total of 50 iterations, over 650 parameter vectors in total. Parameter uncertainty was  
 333 quantified using the parameter vectors, which yielded streamflow estimation performance of  
 334  $NSE \geq 0.5$ , soil moisture estimation performance of  $RMSE \leq 0.05 \text{ m}^3 \text{ m}^{-3}$ , or both. The extent  
 335 of parameter uncertainty associated with each parameter was then scaled from 0-100 using the  
 336 initial parameter range and the equation given below. Normalized parameter uncertainty ( $P_n$ )  
 337 provides an equal scale for comparison across parameters (Kumar & Merwade, (2009) and  
 338 Rajib & Merwade, (2016):

$$339 \quad P_n = \left( \frac{Po - R_{min}}{R_{max} - R_{min}} \right) * 100 \quad (2)$$

340 Where,  $Po$  is parameter value from parameters vectors which fulfilled the selection criteria,  
 341 and  $R_{min/max}$  are initial parameter ranges.

### 342 3 RESULTS

343 Table 1 presents the model sensitivity and calibration results. As described previously, the soil  
 344 depth parameter is not calibrated but rather was adjusted during the model initialization; this  
 345 ensured equivalent comparison between observed and simulated soil moisture (Table 1). As  
 346 explained in section 2.5.2, the CN2 parameter adjustment factors were updated in each iteration  
 347 based on the watershed average CN2 estimate, and the method presented in Easton et.al.  
 348 (2008). The adjustment factors distributed the watershed level storage deficit to local storage  
 349 deficit following TI classification of HRUs. Parameters controlling runoff processes and soil  
 350 properties (CN2, Bulk Density, Available Water Content (AWC), ESCO, Saturated Hydraulic





Conductivity (Ksat), EPCO) in Table 1, were found to be influential across calibration approaches, while parameters controlling baseflow process were less influential. Calibration of the CN2 and Bulk Density parameters resulted in similar values across calibration approaches, while AWC, ESCO, Ksat and EPCO were substantially different.

Table 1: Model parameter sensitivity rank, initial range, and calibrated values.

Parameter	Description	Method	Range		§ SR	¶ Calibrated value		
			min	max		SF	DSM	MO
CN2	Runoff curve number of moisture condition II	replace	40	70	1	42.0	46.7	41.4
Depth	Soil depth	multiply	0.3	3	2	† NC	† NC	† NC
Bulk Density	Soil bulk density	multiply	0.5	1.5	3	0.93	1.22	1.13
‡ SMFMN	Snow melt factor minimum	replace	0	5	4	<u>4.50</u>	<u>4.50</u>	<u>4.50</u>
AWC	Available water content	multiply	0.3	3	5	2.55	1.5	2.7
‡ SMFMX	Snow melt factor maximum	replace	0	5	6	4.50	4.50	4.50
ESCO	Soil evaporation compensation factor	replace	0.1	1	7	0.11	0.69	0.34
Ksat	Saturated hydraulic conductivity	multiply	0.3	3	8	2.36	1.55	2.92
EPCO	Plant evaporation compensation factor	replace	0	1	9	0.94	0.77	0.85
‡ TIMP	Snowpack temperature lag factor	replace	0.01	1	10	<u>0.01</u>	<u>0.01</u>	<u>0.01</u>
‡ SFTMP	Snow fall temperature	replace	-5	5	11	<u>4.00</u>	<u>4.00</u>	<u>4.00</u>
‡ SMTMP	Snow melt temperature	replace	-5	5	12	<u>2.00</u>	<u>2.00</u>	<u>2.00</u>
GW_DELAY	Ground water delay (days)	replace	1	7	13	5.85	3.59	5.3
ALPHA_BF	Baseflow alpha factor (days)	replace	0.12	0.30	14	0.25	0.18	0.26
GWQMN	Threshold depth of water in the shallow aquifer required for return flow initiation (mm)	replace	10	500	15	417	213	494
GW_REVAP	Groundwater “revap” coefficient	replace	0.01	0.05	16	0.04	0.03	0.05
REVAPMN	Threshold depth of water in the shallow aquifer for “revap” initiation (mm)	replace	500	1000	17	996	813	649
RCHRG_DP	Recharges to deep aquifer (fraction)	replace	0.25	0.35	18	0.34	0.33	0.32
SURLAG	Surface runoff lag coefficient	replace	0	15	19	5.15	3.3	4.5

† Not Calibrated

‡ Pre-calibrated snow processes parameter values are underlined

§ Sensitivity Ranking

¶ Calibration on streamflow (SF); Calibration on soil moisture (DSM); Calibration multi-objective (MO)

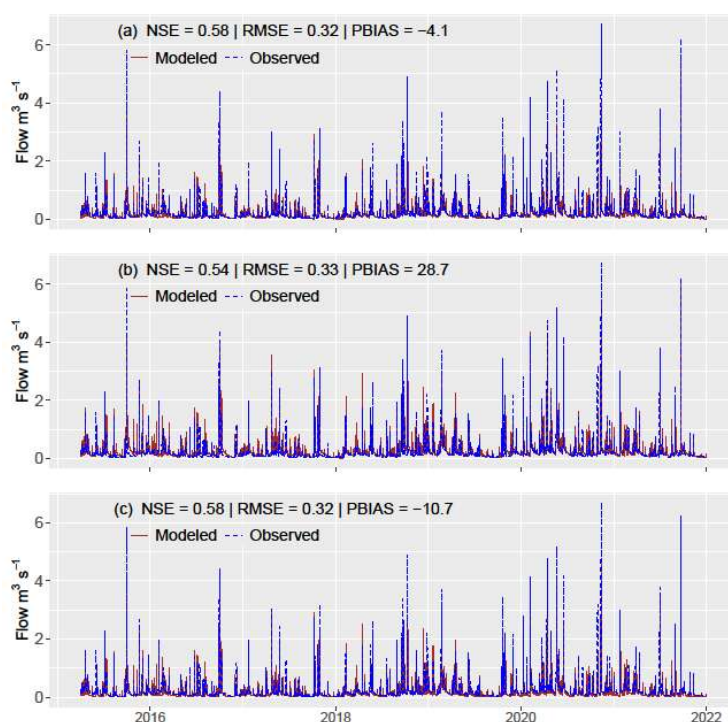


### 361 3.1 Streamflow Calibration

362 The streamflow model calibration was carried out to maximize NSE value and resulted in good  
363 agreement between daily modelled and observed streamflow. After the final calibration, NSE,  
364 RMSE, and PBIAS values were 0.58, 0.32, -4.1%, respectively. As shown in Figure 1, the  
365 streamflow calibrated model captured baseflow well, and while the timing of high flows was  
366 well captured, the model occasionally underestimated peak flows with an overall prediction  
367 bias of -4.1 %. The streamflow calibrated model soil moisture estimates when compared to the  
368 soil moisture data have RMSE,  $R^2$  and NSE values of 0.07, 0.50 and -0.64. The model  
369 explained 50% of the soil moisture variability in the soil moisture data with an RMSE of 0.07.  
370 However, as shown in Fig. 2 and Fig. A3, the timing of the estimated soil moisture peaks was  
371 mismatched as indicated by the poor NSE value.

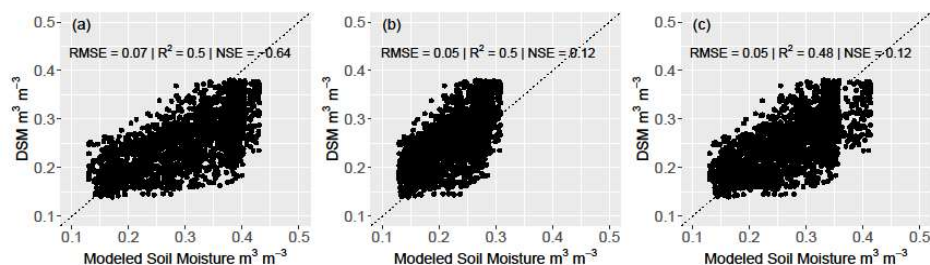
### 372 3.2 Soil Moisture Calibration

373 Soil moisture model calibration was performed to minimize the RMSE between measured and  
374 modeled soil moisture in the 0 - 50 mm soil layer. The calibration resulted in a RMSE value of  
375  $0.05 \text{ m}^3 \text{ m}^{-3}$ . The model explained 50% of the soil moisture variability in the soil moisture data  
376 and improved estimation of the soil moisture peaks with an NSE of 0.12, Figure 2. The model  
377 underestimated soil moisture, as illustrated by proportion of data above the 1:1 line in Fig. 2  
378 and the temporal variability in Fig. A3. The model's daily stream flow estimation performance  
379 was satisfactory with NSE, RMSE, and PBIAS values of 0.54,  $0.03 \text{ m}^3/\text{s}$ , and 28.7 %,  
380 respectively (Figure 1Figure 1), with moderately overestimated low flows, and well predicted  
381 peak flows. The overall bias of the soil moisture only calibration was 28.7%, attributable to  
382 poor low flow prediction.



383

384 Figure 1: Model streamflow prediction performance calibration period a) streamflow only (SF)  
 385 calibration b) soil moisture only (DSM) calibration c) multi-objective (MO) calibration.



386

387 Figure 2: Model soil moisture estimation performance during the calibration period compared  
 388 against downscaled and bias corrected soil moisture data calibrated on a) streamflow only (SF)  
 389 calibration b) soil moisture only (DSM) calibration c) multi-objective (MO) calibration.



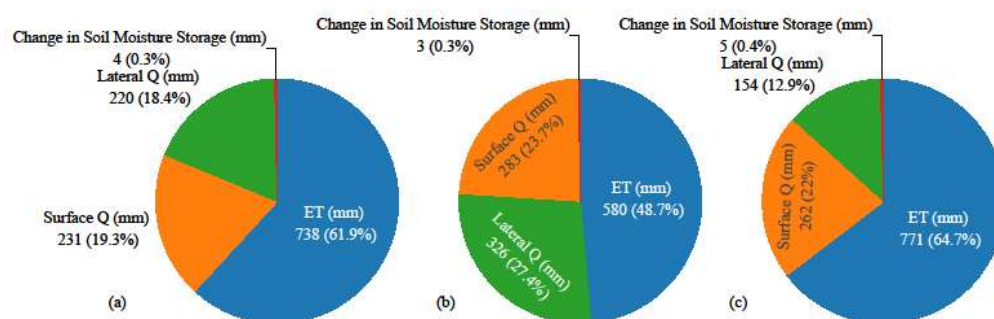
### 390 3.3 Multi-objective Calibration

391 The multi-objective model calibration optimized soil moisture and streamflow simultaneously.  
392 The algorithm returned 14 candidate solutions on a pareto front. Among the candidate models,  
393 the best model was selected based on the performance against in-situ soil moisture  
394 measurements. The parameter values of the multi-objective calibrated model are presented in  
395 Table 1. The model showed satisfactory performance in streamflow estimation with NSE,  
396 RMSE, and PBIAS values of 0.58,  $0.32 \text{ m}^3 \text{ m}^{-3}$ , and  $-10.7 \%$ , respectively, Figure 1.

397 The RMSE,  $R^2$ , and NSE values for soil moisture estimation were  $0.05 \text{ m}^3 \text{ m}^{-3}$ , 0.48, and 0.12,  
398 respectively. The performance shows that the model was able to explain 48% of the soil  
399 moisture variability in the observed soil moisture data. Model soil moisture estimates also  
400 showed better correspondence with measured soil moisture data with improved alignment on  
401 the one-to-one line when compared to the streamflow model, Figure 2.

### 402 3.4 Parameter Estimation and Water Balance Evaluation

403 The CN2 values did not differ substantially between the three models. The average CN2 values  
404 were 42, 41.4, and 46.7 for the streamflow, multi-objective and soil moisture models  
405 respectively, Table 1. This is also evident from the surface runoff component in the water  
406 balance values, which range between 19.3% and 23.7%, Figure 3. Among the three calibration  
407 approaches the soil moisture only calibration resulted in substantially different ET and lateral  
408 flow. The majority of the incoming precipitation returns to the atmosphere in the form of ET  
409 with the remaining water balance eventually contributing to streamflow with little to no deep  
410 percolation.



411  
 412 Figure 3: Model water balance estimation a) streamflow only (SF) calibration b) soil moisture  
 413 only (DSM) calibration c) multi-objective (MO) calibration.

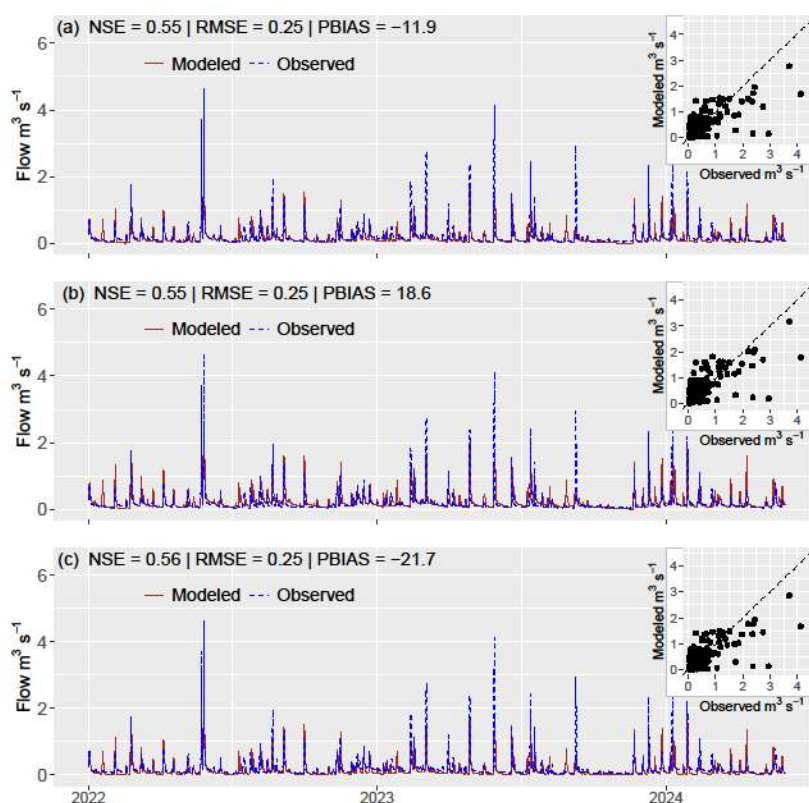
### 414 3.5 Model Evaluation and Comparison

415 During the model evaluation period (01 Jan 2022 – 31 May 2024) all three models showed  
 416 satisfactory streamflow estimation performance with NSE values of 0.55 – 0.56 and RMSE  
 417  $0.25 \text{ m}^3 \text{ m}^{-3}$ , Figure 4. The soil moisture calibrated model showed an over-estimation bias on  
 418 daily streamflow estimation average over the simulation period of 18.6 %, primarily during  
 419 low flows; while streamflow and multi-objective calibrated models showed an under-  
 420 estimation bias of -11.9 and -21.7%, respectively, Figure 4.

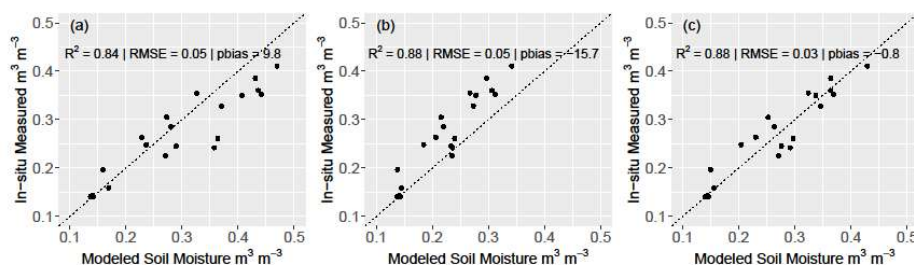
421 The soil moisture measurements are used as the primary data for model performance evaluation  
 422 of soil moisture estimates from each of the models. At the field scale, the performance of the  
 423 three models in estimating soil moisture in the topsoil layer (50mm) is evaluated using RMSE,  
 424  $R^2$ , and PBIAS. The streamflow calibrated model explained 84% of the variability ( $R^2 = 0.84$ ),  
 425 while soil moisture and multi-objective calibrated models explained 88% of the soil moisture  
 426 variability ( $R^2 = 0.88$ ), Fig. 5. The streamflow calibrated model over-predicted moderate to  
 427 high soil moisture conditions while the soil moisture calibrated model under predicted, Fig. 6.



428 The multi-objective calibration reduced RMSE of model estimated soil moisture compared to  
 429 the stream flow only and soil moisture only calibrated models from  $0.05 \text{ m}^3 \text{ m}^{-3}$  to  $0.03 \text{ m}^3 \text{ m}^{-3}$   
 430 <sup>3</sup> and PBIAS from 9.8 and -15.7 to -0.8, Fig. 5. The time series plot, Fig. 6, also shows that the  
 431 streamflow calibrated model performs better for low soil moisture conditions compared to high  
 432 soil moisture conditions.

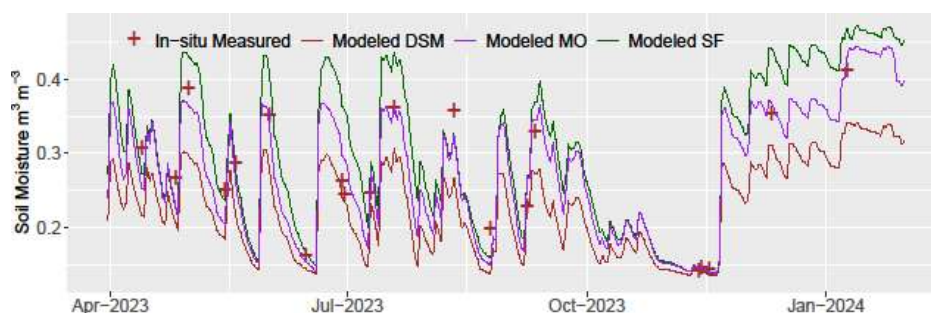


433  
 434 Figure 4: Model streamflow estimation performance evaluation period a) streamflow only (SF)  
 435 calibration b) soil moisture only (DSM) calibration c) multi-objective (MO) calibration.



436

437 Figure 5: Soil moisture estimation performance of the three models in the evaluation period at  
 438 field scale against field scale average soil moisture estimate from in-situ measurements.



439

440 Figure 6: Temporal variability of modeled and measured soil moisture for the three calibration  
 441 approaches average over the top 120mm soil layer; streamflow only (SF), soil moisture only  
 442 (DSM), and Multi-objective (MO).

## 443 4 DISCUSSION

### 444 4.1 Streamflow Calibration

445 The streamflow only calibration yielded a satisfactory NSE of 0.58. A slightly better NSE value  
 446 of 0.60 was reported for streamflow by Thilakarathne et al., (2018) although they used only a  
 447 2- year stream flow record for model calibration and perhaps their model may not have seen a  
 448 wide range of variability in streamflow compared to our calibration using ~10- year flow





449 record. Streamflow calibrated parameter values are presented in Table 1. Parameters describing  
450 soil properties - Bulk Density, AWC, and Ksat - increased from values in the soils database by  
451 -7%, 155% and 136%, respectively. Indeed, Buell, (2022) and Fuka et al. (2016) showed that  
452 large scale soil databases may not be representative of local soil properties such as texture,  
453 horizon thickness, and organic matter content. Therefore, allowing more variation in soil  
454 properties parameters during calibration is justified.

#### 455 4.2 Soil Moisture Calibration

456 Calibrating the model on soil moisture improved the model's soil moisture performance but  
457 slightly reduced streamflow performance for the calibration period, Fig. 1. Reductions in  
458 streamflow performance when calibrating soil moisture are reported in several studies (Dangol  
459 et al., 2023; Kofidou & Gemitzi, 2023). However, the scales of the reductions are different.  
460 Kofidou & Gemitzi, (2023) reported a reduction in NSE from 0.58 to 0.51. In contrast, Dangol  
461 et al. (2023) reported a decline in the model streamflow performance with the NSE declining  
462 from 0.56 to -0.22. These inconsistencies in reported model performance can emanate from the  
463 type and resolution of satellite data used in the study, the data preprocessing steps such as bias  
464 correction, model structure and resolution, or from the runoff generation mechanism in the  
465 watershed, and soil moisture variability. Dangol et al. (2023) attributed poor model  
466 performance to the quality of remotely sensed products and suggested careful assessment.  
467 Here, we note that preprocessing bias using effective precipitation as described in the methods  
468 improved the performance of the downscaled soil moisture data for model calibration.





#### 469 4.3 Multi-objective Calibration

470 The multi-objective calibrated model showed satisfactory performance for both streamflow and  
471 soil moisture estimation. The multi-objective model also showed greater temporal variability  
472 compared to the soil moisture only model, Fig. A3. This may be related to improved parameter  
473 estimation, as multi-objective calibration constrains parameters controlling both soil moisture  
474 and streamflow processes simultaneously. Overall, the multi-objective calibrated model was  
475 able to match the performance of the streamflow only calibrated model for streamflow  
476 estimation and the performance of soil moisture only calibrated model for soil moisture  
477 estimation.

478 Investigating the utility of multi-objective calibration in hydrological modeling using soil  
479 moisture, evapotranspiration, and surface runoff products on 20 watersheds in the lake  
480 Michigan watershed, Mei et al. (2023) found that multi-objective calibration improved model  
481 performance for evapotranspiration, soil moisture, or surface runoff but with a reduction in  
482 streamflow performance compared to model calibrated on streamflow only. Duethmann et al.  
483 (2022) also reported improvement in soil moisture estimation with a concurrent reduction in  
484 streamflow performance as compared to a streamflow only calibrated model. Mei et al. (2023)  
485 noted the reduction in streamflow estimation performance was the least when using soil  
486 moisture compared to when using ET or runoff products in addition to streamflow. In addition  
487 both Duethmann et al. (2022) and Mei et al. (2023) reported model calibration on streamflow  
488 and soil moisture improved ET simulation as well, which Mei et al. (2023) attributed to  
489 improved representation of soil moisture variability in the multi-objective model while  
490 Duethmann et al. (2022) attributed it simply to difference in parameter values. Their findings  
491 are in line with our results except streamflow performance of the multi-objective model is



492 equivalent to the streamflow model with a slight increase in bias. Other studies have also  
493 reported similar findings using multi-objective calibration with varying degrees of success on  
494 soil moisture estimation performance and corresponding reduction in streamflow estimation  
495 performance as compared to model calibrated on streamflow only (Kofidou & Gemitzi, 2023;  
496 Rajib et al., 2016). Comparing results across studies requires caution, as satellite soil moisture  
497 products differ in sensing depth, resolution, and post-processing. Additionally, most studies  
498 use distinct scaling and smoothing methods, such as the soil water index (Wagner et al., 1999),  
499 to align satellite data with reference soil depths or in-situ measurements.

500 In the multi-objective calibration, model parameters were selected based on model  
501 performance defined on objective functions optimizing both streamflow and soil moisture.  
502 Theoretically, given adequate temporal and spatial resolution, model structure, and the  
503 calibration approach, the measured soil moisture data could be expected to complement the  
504 streamflow data by constraining the antecedent moisture conditions (Brocca et al., 2017;  
505 Wagner et al., 2007). This leads to improved prediction of both soil moisture and streamflow.  
506 In this regard, the bias correction approach, based on effective precipitation, used to enhance  
507 the temporal fluctuation of the soil moisture data may have aided in improved model estimation  
508 of both streamflow and soil moisture.

#### 509 4.4 Parameter Estimation and Water Balance Evaluation

510 The CN2 values for TI class 1 (18.3 to 22.3), when distributed using the adjustment factors  
511 discussed in the methods, indicate that areas under TI class 1 contribute very little to surface  
512 runoff, TI class 1 covers 56% of the watershed area but generates only 9% of watershed runoff  
513 per unit area. At the calibrated CN2 values, TI class 3, 6% of the watershed area generates



514 ~30% of total surface runoff. This is not unusual for saturation excess dominated watersheds,  
515 where surface runoff occurs on low lying and converging planform areas of limited spatial  
516 extent that receive subsurface moisture flux from upslope areas (Dahlke et al., 2009; Easton et  
517 al., 2008; Lyon et al., 2004). Soil moisture variability due to surface and subsurface flux  
518 exchange in the watershed is indirectly estimated by distributing CN2 values according to the  
519 local storage deficit (Dahlke et al., 2009; Easton et al., 2008). The SURLAG (surface runoff  
520 lag time) coefficient for the streamflow only calibrated model is higher than the values for the  
521 soil moisture and multi-objective calibrated models, yet this difference has a small effect in  
522 delaying surface runoff from reaching the stream outlet as the time of concentration in these  
523 watersheds is less than 1.5 hrs.

524 The difference in ET and lateral flow components in the soil moisture only calibrated model as  
525 compared to the other two models may be due to the reduced soil moisture variability and  
526 reduced AWC in the soil moisture only calibration, which had a lower mean and coefficient of  
527 variation (CV), compared to soil moisture estimate from the streamflow and multi-objective  
528 calibrated models, Table 2. Although the soil bulk density was high for soil moisture  
529 calibration, Table 1, which compensated for reduced AWC via reductions in soil porosity;  
530 looking at Fig. A3 and Fig. 6 it was clear that soil moisture remained mostly under  $0.40 \text{ m}^3 \text{ m}^{-3}$   
531 for all models. This indicates that higher porosity values in the streamflow only and multi-  
532 objective calibrated models were less frequently activated for moisture storage. Mean, standard  
533 deviation, and CV values for soil moisture estimates of the three models are presented in Table  
534 2. The lowest mean and CV values were for the soil moisture only calibrated model, which was  
535 comparable to the measured soil moisture data but less similar to the estimates from the  
536 streamflow calibrated model. When calibrating on streamflow, only the algorithm allows for



greater variability in soil moisture related parameters because streamflow has higher CV compared to soil moisture. In contrast, the soil moisture model calculates objective function changes directly on soil moisture estimates and is thereby influenced by the characteristics of the soil moisture data.

Other parameters that affect ET such as ESCO and EPCO had more effect on the multi-objective calibrated model where both parameters force more ET from lower soil layers, Table 1. Unsaturated moisture flux between soil layers is indirectly modeled in SWAT using two equations controlled by the ESCO and EPCO parameters (Neitsch et al., 2009). The soil moisture model has both ESCO and EPCO close to 1 compensating each other – that is EPCO allows for more ET to be accessed from lower soil layers and ESCO allows for less, while for streamflow and multi-objective calibrated models both parameters allow more ET to come from lower soil layers, Table 1. Groundwater and baseflow parameters have little effect on the results with close to zero percolation estimated across all three models.

Table 2: Soil moisture variability during the calibration period observed and modeled.

Soil Moisture	Mean	Standard Deviation	Coefficient of Variation
Soil moisture data	0.26	0.06	22.4
From streamflow model	0.31	0.08	26.9
From soil moisture model	0.23	0.05	21.8
From multi-objective model	0.28	0.07	24.8

#### 4.5 Model Evaluation and Comparison

Similar to findings in other studies incorporating soil moisture in model calibration improved soil moisture estimation, for example, Duethmann et al. (2022), Kofidou & Gemitzi, (2023), and Rajib et al. (2016) showed multi-objective calibration improved model soil moisture estimation performance when compared to streamflow only calibrated models. In contrast,



556 Dangol et al. (2023) reported that the use of multi-objective calibration (streamflow with  
557 satellite products) did not necessarily improve overall model performance. Our result suggests  
558 that multi-objective calibration improved soil moisture predictions substantially without  
559 deteriorating streamflow estimates.

560 The original SMAP mission objectives were to achieve a RMSE of  $0.04 \text{ m}^3 \text{ m}^{-3}$  or less at  
561 original mission resolution (Colliander et al., 2017; Entekhabi et al., 2014). The product used  
562 in this study is reported to meet an RMSE of  $0.08 \text{ m}^3 \text{ m}^{-3}$  against in-situ measurement at the  
563 downscaled resolution (Peng et al., 2024). Although, the in-situ measurements used in this  
564 study do not overlap in time with the mlhrsm downscaled SMAP mission data affording no  
565 direct evaluation – the multi-objective calibration of SWAT-VSA model using soil moisture  
566 data improved the modeled soil moisture estimates at the field scale, Fig. 5 and Fig. 6. All three  
567 models underestimated peak flows during the evaluation period. This may be due to the quality  
568 of the precipitation data used or due to the presence of substantial urban/impervious surfaces  
569 in the watershed, which are typically less well simulated by SWAT.

#### 570 4.6 Parameter uncertainty

571 Among the advantages of multi-objective calibration reported in previous studies was the  
572 reduction of parameter uncertainty (Kundu et al., 2017; Rajib et al., 2016; Silvestro et al.,  
573 2015). Equifinality is a well-known problem in model calibration where combinations of  
574 different parameter values may result in equally plausible objective function solutions (Beven,  
575 1993). To evaluate parameter uncertainty across the calibration approaches a normalized  
576 uncertainty score was calculated using Eq. (2), Fig. 7. Using this approach, a wider range or  
577 spread in parameter values indicates higher uncertainty – i.e. as the iterative search space for



the optimum parameter value widens the possibility of the optimization algorithm arriving at several equally performing solutions increases, Fig. 7. In other words, the algorithm required a wider range of parameter values to find a satisfactory solution.

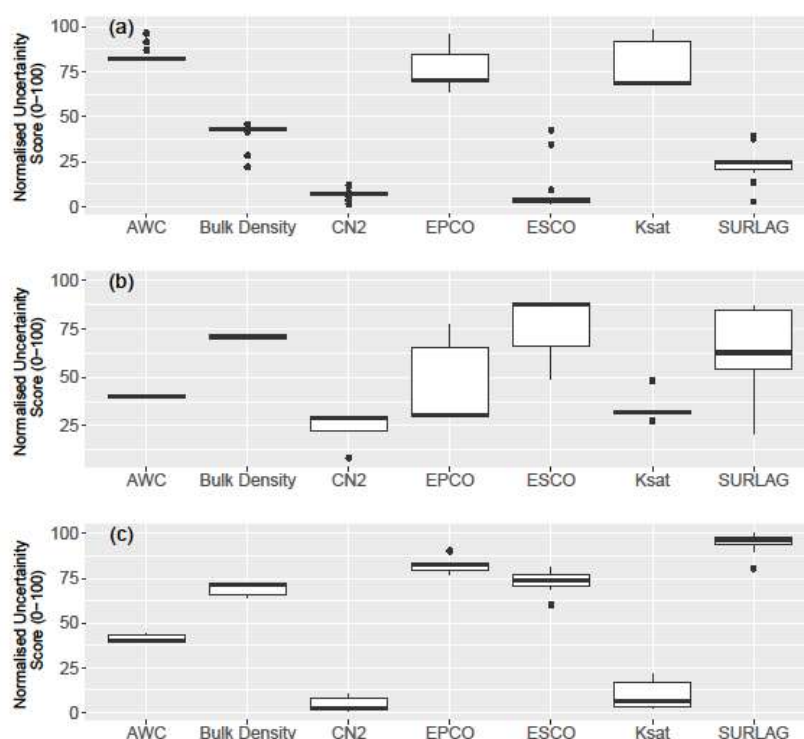


Figure 7: Parameter uncertainty estimate derived from DEoptim calibration iterations for the models calibrated on a) streamflow only, b) soil moisture only and, c) multi-objective calibration. The height of the boxplot demonstrates the range of different values the parameters took while yielding acceptable model performance. The values are calculated using normalized uncertainty score (Kumar & Merwade, 2009). Where 0 and 100 represent the minimum and maximum parameter value as defined by the normalized calibration range.



588 The AWC, Bulk Density, and Ksat parameters show lower relative uncertainty when soil  
589 moisture is part of the calibration objective. This is not surprising as these parameters directly  
590 impact the soil moisture state, Fig. 7b and Fig. 7c. Moreover, the values the parameter take  
591 within the calibration range are different than when calibrating on streamflow only, for  
592 example, Ksat takes high values for streamflow only calibration and low values for the other  
593 two within the calibration range – hence the extent to which the parameters affect model  
594 behavior is different for soil moisture and streamflow calibration. CN2 and SURLAG have the  
595 lowest uncertainty, demonstrated by the height of the boxplot, when streamflow is part of the  
596 calibration objective, Fig. 7a and Fig. 7c. This is not unexpected, as AWC, Bulk Density, and  
597 Ksat have a stronger influence on soil moisture, while CN2 and SURLAG influence streamflow  
598 to a greater extent. Overall, parameter estimation uncertainty is reduced when using the multi-  
599 objective calibration approach similar to findings in Rajib & Merwade, (2016) and Silvestro et  
600 al. (2015) – this was likely because the parameters were constrained on multiple objectives,  
601 which limited the possibility for inter-parameter compensation. Other parameters, such as  
602 EPCO and ESCO, although not physically based, also display substantially reduced uncertainty  
603 under multi-objective calibration.

## 604 5 CONCLUSIONS

605 This study evaluated the utility of downscaled satellite soil moisture data for calibrating a  
606 SWAT-VSA model in a small watershed for enhanced estimation of field scale soil moisture  
607 variability. The results showed leveraging downscaled satellite soil moisture data substantially  
608 improved estimation of temporal variability of soil moisture without deteriorating the model  
609 accuracy in streamflow estimation. In comparison, multi-objective calibration using

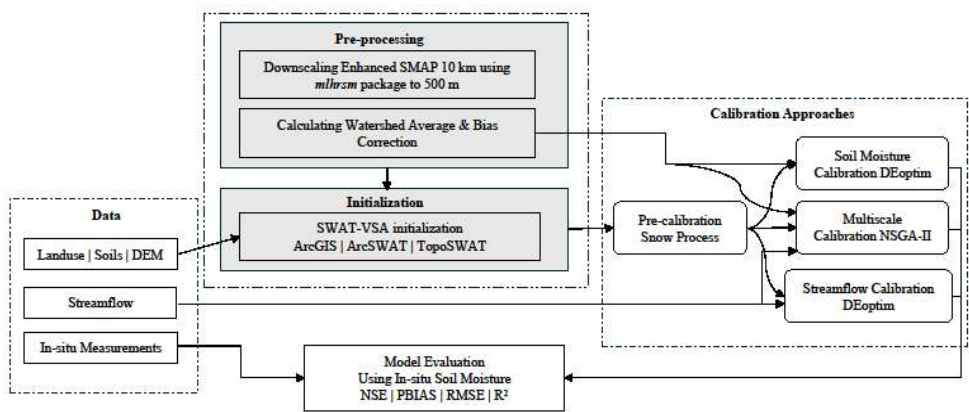


610 streamflow and satellite soil moisture improved overall model performance both in estimating  
611 streamflow and soil moisture more than calibration individually for streamflow and soil  
612 moisture. The model calibrated on soil moisture only showed minimal decline in streamflow  
613 estimation performance for the calibration and evaluation period compared to the model  
614 calibrated on streamflow only. It also resulted in improved soil moisture estimation  
615 performance. Machine learning based satellite soil moisture downscaling, using the ‘mlrhm’  
616 package in R, provided adequate data to calibrate a high-resolution SWAT-VSA model in a  
617 small watershed. Parameter uncertainty varied with calibration data and the calibration  
618 approach, soil parameters were better constrained with soil moisture data, and streamflow  
619 parameters with streamflow data. Multi-objective calibration reduced parameter uncertainty.  
620 Additional investigation is required to replicate this approach in diverse watersheds as well as  
621 evaluating both surface and deep layer soil moisture performance. Long-term water balance  
622 estimates varied widely across the three calibration approaches. Further investigation, for  
623 example using in-situ ET measurement, is needed to assess how soil moisture data influences  
624 watershed water balance components. The findings in this study have implications for use of  
625 watershed models in ungauged basins for both streamflow and soil moisture estimation. This  
626 is particularly significant as remotely sensed satellite soil moisture products have global  
627 coverage.

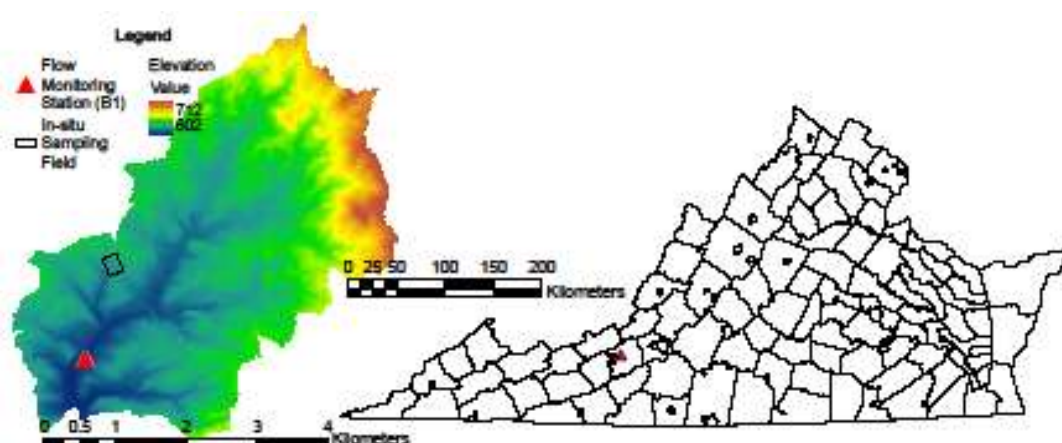




628 APPENDICES



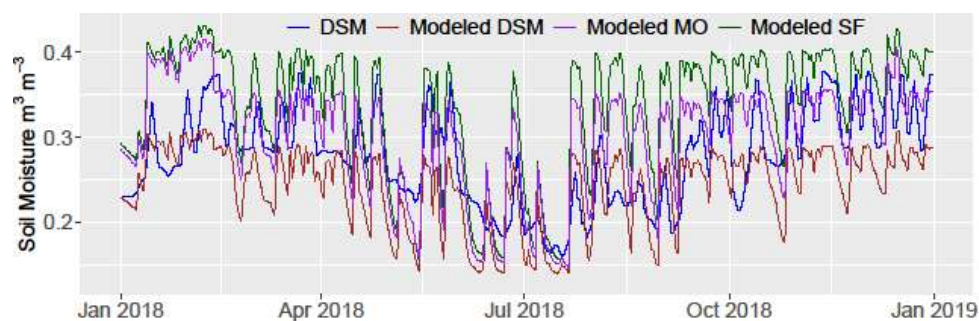
629  
630 Fig. A1: General workflow of the data pre-processing, model calibration and model  
631 performance evaluation.



640

641 Fig. A2: Location map of the Stroubles Creek

642



643

644 Fig. A3: Time series of modeled surface soil moisture (50 mm) from the three calibration  
 645 approaches and DSM data; calibrated on DSM data (Modeled DSM), Multi-objective  
 646 calibration using DSM data and streamflow (Modeled MO), calibrated on streamflow  
 647 (Modeled SF).

648



649    **CODE AVAILABILITY**

650    The code used to run the simulations is available in a GitHub repository.

651    [https://github.com/saizanaandezana/Stroubles\\_Creek\\_SWAT\\_VSA\\_model](https://github.com/saizanaandezana/Stroubles_Creek_SWAT_VSA_model)

652    **DATA AVAILABILITY**

653    The majority of the data used in this study is publicly available.

654    **TEAM LIST**

655    Binyam Workeye Asfaw; Siam Maksud; Daniel R. Fuka; Amy S. Collick; Robin R. White;

656    Zachary M. Easton

657    **AUTHOR CONTRIBUTION**

658    Binyam Workeye Asfaw: Conceptualization; data curation; formal analysis; investigation;  
659    methodology; visualization; writing—original draft; writing—review and editing.

660    Siam Maksud: Data curation; writing—review and editing.

661    Daniel R. Fuka: Conceptualization; methodology; writing—review and editing.

662    Amy S. Collick: Methodology; writing-review and editing

663    Robin R. White: Conceptualization; funding acquisition; project administration.

664    Zachary M. Easton: Conceptualization; data curation; formal analysis; funding acquisition;  
665    project administration; writing—original draft; writing—review and editing.



666   COMPETING INTERESTS

667   Authors declare that they have no competing interest.

668   ACKNOWLEDGEMENTS

669   We acknowledge USDA CPS for the financial support.

670   FINANCIAL SUPPORT

671   This research was funded by USDA CPS award number 2021-67021-34769.

672   REFERENCES

673   Abbaszadeh, P., Moradkhani, H., Gavahi, K., Kumar, S., Hain, C., Zhan, X., Duan, Q., Peters-  
674       Lidard, C., & Karimiziarani, S. (2021). High-resolution SMAP satellite soil moisture  
675       product: Exploring the opportunities. *Bulletin of the American Meteorological Society*,  
676       102(4), 309–315.

677   Arnold, J. G., Moriasi, D. N., Gassman, P. W., Abbaspour, K. C., White, M. J., Srinivasan, R.,  
678       Santhi, C., Harmel, R. D., Van Griensven, A., & Van Liew, M. W. (2012). SWAT:  
679       Model use, calibration, and validation. *Transactions of the ASABE*, 55(4), 1491–1508.

680   Asfaw, B. W., Fuka, D. R., Collick, A. S., White, R. R., & Easton, Z. M. (2025). Characterizing  
681       the topographic index as a tool to represent spatial soil moisture: The effect of  
682       classification approach, digital elevation model type, and resolution. *Vadose Zone*  
683       *Journal*, 24(4), e70031. <https://doi.org/10.1002/vzj2.70031>

684   Azimi, S., Dariane, A. B., Modanesi, S., Bauer-Marschallinger, B., Bindlish, R., Wagner, W.,  
685       & Massari, C. (2020). Assimilation of Sentinel 1 and SMAP – based satellite soil



- 686 moisture retrievals into SWAT hydrological model: The impact of satellite revisit time  
 687 and product spatial resolution on flood simulations in small basins. *Journal of*  
 688 *Hydrology*, 581. <https://doi.org/10.1016/j.jhydrol.2019.124367>
- 689 Bekele, E. G., & Nicklow, J. W. (2007). Multi-objective automatic calibration of SWAT using  
 690 NSGA-II. *Journal of Hydrology*, 341(3), 165–176.  
 691 <https://doi.org/10.1016/j.jhydrol.2007.05.014>
- 692 Beven, K. J., Kirkby, M. J., Freer, J. E., & Lamb, R. (2021). A history of TOPMODEL.  
 693 *Hydrology and Earth System Sciences*, 25(2), 527–549. [https://doi.org/10.5194/hess-](https://doi.org/10.5194/hess-25-527-2021)  
 694 25-527-2021
- 695 Blank, J., & Deb, K. (2020). Pymoo: Multi-Objective Optimization in Python. *IEEE Access*, 8,  
 696 89497–89509. IEEE Access. <https://doi.org/10.1109/ACCESS.2020.2990567>
- 697 Bocinsky, R. K., Beaudette, D., Chamberlain, S., Hollister, J., & Gustavsen, J. (2025).  
 698 *FedData: Download Geospatial Data Available from Several Federated Data Sources*  
 699 (Version 4.3.0). <https://cran.r-project.org/web/packages/FedData/index.html>
- 700 Brocca, L., Ciabatta, L., Massari, C., Camici, S., & Tarpanelli, A. (2017). Soil Moisture for  
 701 Hydrological Applications: Open Questions and New Opportunities. *Water*, 9(2), 2.  
 702 <https://doi.org/10.3390/w9020140>
- 703 Brocca, L., Melone, F., Moramarco, T., & Morbidelli, R. (2010). Spatial-temporal variability  
 704 of soil moisture and its estimation across scales. *Water Resources Research*, 46(2).  
 705 <https://doi.org/10.1029/2009WR008016>



- 706 Buell, E. N. (2022). *Improved Environmental Characterization to Support Natural Resource*  
 707 *Decision Making: (1) Distributed Soil Characterization, and (2) Treatment of Legacy*  
 708 *Nutrients*. <http://hdl.handle.net/10919/112013>
- 709 Chan, S. K., Bindlish, R., O'Neill, P., Jackson, T., Njoku, E., Dunbar, S., Chaubell, J.,  
 710 Piepmeier, J., Yueh, S., Entekhabi, D., Colliander, A., Chen, F., Cosh, M. H., Caldwell,  
 711 T., Walker, J., Berg, A., McNairn, H., Thibeault, M., Martínez-Fernández, J., Uldall,  
 712 F., Seyfried, M., Bosch, D., Starks, P., Holifield Collins, C., Prueger, J., Van Der Velde,  
 713 R., Asanuma, J., Palecki, M., Small, E. E., Zreda, M., Calvet, J., Crow, W. T., & Kerr,  
 714 Y. (2018). Development and assessment of the SMAP enhanced passive soil moisture  
 715 product. *Remote Sensing of Environment*, 204, 931–941.  
 716 <https://doi.org/10.1016/j.rse.2017.08.025>
- 717 Cho, E., Moon, H., & Choi, M. (2015). First Assessment of the Advanced Microwave Scanning  
 718 Radiometer 2 (AMSR2) Soil Moisture Contents in Northeast Asia. *Journal of*  
 719 *Meteorology. Series 2*, 93(1), 117–129. <https://doi.org/10.2151/jmsj.2015-008>
- 720 Colliander, A., T.J. Jackson, R. Bindlish, S. Chan, N. Das, S.B. Kim, M.H. Cosh, R.S. Dunbar,  
 721 L. Dang, L. Pashaian, J. Asanuma, K. Aida, A. Berg, T. Rowlandson, D. Bosch, T.  
 722 Caldwell, K. Caylor, D. Goodrich, H. al Jassar, E. Lopez-Baeza, J. Martínez-Fernández,  
 723 A. González-Zamora, S. Livingston, H. McNairn, A. Pacheco, M. Moghaddam, C.  
 724 Montzka, C. Notarnicola, G. Niedrist, T. Pellarin, J. Prueger, J. Pulliainen, K.  
 725 Rautiainen, J. Ramos, M. Seyfried, P. Starks, Z. Su, Y. Zeng, R. van der Velde, M.  
 726 Thibeault, W. Dorigo, M. Vreugdenhil, J.P. Walker, X. Wu, A. Monerris, P.E. O'Neill,  
 727 D. Entekhabi, E.G. Njoku, & S. Yueh. (2017). Validation of SMAP surface soil



- 728 moisture products with core validation sites. *Remote Sensing of Environment*, 191, 215–  
 729 231. <https://doi.org/10.1016/j.rse.2017.01.021>
- 730 Dahlke, H. E., Easton, Z. M., Fuka, D. R., Lyon, S. W., & Steenhuis, T. S. (2009). Modelling  
 731 variable source area dynamics in a CEAP watershed. *Ecohydrology*, 2(3), 337–349.  
 732 <https://doi.org/10.1002/eco.58>
- 733 Dangol, S., Zhang, X., Liang, X.-Z., Anderson, M., Crow, W., Lee, S., Moglen, G. E., &  
 734 Mccarty, G. W. (2023). Multivariate Calibration of the SWAT Model Using Remotely  
 735 Sensed Datasets. *Remote Sensing*, 2417 (22 pp.). <https://doi.org/10.3390/rs15092417>
- 736 Das, N. N., Entekhabi, D., Kim, S., Jagdhuber, T., Dunbar, S., Yueh, S., O'Neill, P. E.,  
 737 Colliander, A., Walker, J., & Jackson, T. J. (2018). High-resolution enhanced product  
 738 based on SMAP active-passive approach using sentinel 1A and 1B SAR data.  
 739 *International Archives of the Photogrammetry, Remote Sensing and Spatial*  
 740 *Information Sciences.*, XLII–5, 203–205. [https://doi.org/10.5194/isprs-archives-XLII-](https://doi.org/10.5194/isprs-archives-XLII-5-203-2018)  
 741 [5-203-2018](https://doi.org/10.5194/isprs-archives-XLII-5-203-2018)
- 742 De Santis, D., Biondi, D., Crow, W. T., Camici, S., Modanesi, S., Brocca, L., & Massari, C.  
 743 (2021). Assimilation of satellite soil moisture products for river flow prediction: An  
 744 extensive experiment in over 700 catchments throughout europe. *Water Resources*  
 745 *Research*, 57(6). <https://doi.org/10.1029/2021WR029643>
- 746 Deb, K., Agrawal, S., Pratap, A., & Meyarivan, T. (2000). A Fast Elitist Non-dominated  
 747 Sorting Genetic Algorithm for Multi-objective Optimization: NSGA-II. In M.  
 748 Schoenauer, K. Deb, G. Rudolph, X. Yao, E. Lutton, J. J. Merelo, & H.-P. Schwefel



- 749 (Eds.), *Parallel Problem Solving from Nature PPSN VI* (pp. 849–858). Springer.  
 750 [https://doi.org/10.1007/3-540-45356-3\\_83](https://doi.org/10.1007/3-540-45356-3_83)
- 751 Duethmann, D., Smith, A., Soulsby, C., Kleine, L., Wagner, W., Hahn, S., & Tetzlaff, D.  
 752 (2022). Evaluating satellite-derived soil moisture data for improving the internal  
 753 consistency of process-based ecohydrological modelling. *Journal of Hydrology*, 614,  
 754 128462. <https://doi.org/10.1016/j.jhydrol.2022.128462>
- 755 Easton, Z. M., Fuka, D. R., Walter, M. T., Cowan, D. M., Schneiderman, E. M., & Steenhuis,  
 756 T. S. (2008). Re-conceptualizing the soil and water assessment tool (SWAT) model to  
 757 predict runoff from variable source areas. *Journal of Hydrology*, 348(3), 279–291.  
 758 <https://doi.org/10.1016/j.jhydrol.2007.10.008>
- 759 Eini, M. R., Massari, C., & Piniewski, M. (2023). Satellite-based soil moisture enhances the  
 760 reliability of agro-hydrological modeling in large transboundary river basins. *Science*  
 761 *of The Total Environment*, 873, 162396.  
 762 <https://doi.org/10.1016/j.scitotenv.2023.162396>
- 763 Entekhabi, D., Reichle, R. H., Koster, R. D., & Crow, W. T. (2010). *Performance Metrics for*  
 764 *Soil Moisture Retrievals and Application Requirements*.  
 765 <https://doi.org/10.1175/2010JHM1223.1>
- 766 Entekhabi, D., Yueh, Si., & De Lannoy, G. (2014). *SMAP handbook*.
- 767 Food and Agriculture Organization of the United Nations (FAO). (2007). *FAO Digital Soil*  
 768 *Map of the World (DSMW)*. [https://www.fao.org/land-water/land/land-](https://www.fao.org/land-water/land/land-governance/land-resources-planning-toolbox/category/details/en/c/1026564/)  
 769 [governance/land-resources-planning-toolbox/category/details/en/c/1026564/](https://www.fao.org/land-water/land/land-governance/land-resources-planning-toolbox/category/details/en/c/1026564/)





- 770 Fuka, D. R., Collick, A. S., Kleinman, P. J. A., Auerbach, D. A., Harmel, R. D., & Easton, Z.  
 771 M. (2016). Improving the spatial representation of soil properties and hydrology using  
 772 topographically derived initialization processes in the SWAT model. *Hydrological*  
 773 *Processes*. <https://doi.org/10.1002/hyp.10899>
- 774 Fuka, D. R., & Easton, Z. M. (2016). *TopoSWAT Source. Figshare. Dataset.*  
 775 <https://doi.org/10.6084/m9.figshare.1342823.v4>.
- 776 Fuka, D. R., W, M., A, J., Garna, R. K., & Easton, Z. M. (2013). *EcoHydRology: A community*  
 777 *modeling foundation for EcoHydrology* (Version R package version 0.4.19 [software]).  
 778 <https://CRAN.R-project.org/package=EcoHydRology>
- 779 Garna, R. K., Easton, Z. M., Faulkner, J. W., Collick, A. S., & Fuka, D. R. (2023). Employing  
 780 higher density lower reliability weather data from the Global Historical Climatology  
 781 Network monitors to generate serially complete weather data for watershed modelling.  
 782 *Hydrological Processes*, 37(11), e15013. <https://doi.org/10.1002/hyp.15013>
- 783 H SAF. (2021). *ASCAT Surface Soil Moisture Climate Data Record v7 12.5 km sampling—*  
 784 *Metop, EUMETSAT SAF on Support to Operational Hydrology and Water*  
 785 *Management*. [https://doi.org/10.15770/EUM\\_SAF\\_H\\_0009](https://doi.org/10.15770/EUM_SAF_H_0009)
- 786 Han, L., Wang, C., Liu, Q., Wang, G., Yu, T., Gu, X., & Zhang, Y. (2020). Soil Moisture  
 787 Mapping Based on Multi-Source Fusion of Optical, Near-Infrared, Thermal Infrared,  
 788 and Digital Elevation Model Data via the Bayesian Maximum Entropy Framework.  
 789 *Remote Sensing*, 12(23). <https://doi.org/10.3390/rs12233916>



- 790 Hofmeister, K. L., Cianfrani, C. M., & Hession, W. C. (2015). Complexities in the stream  
 791 temperature regime of a small mixed-use watershed, Blacksburg, VA. *Ecological*  
 792 *Engineering*, 78, 101–111. <https://doi.org/10.1016/j.ecoleng.2014.05.019>
- 793 Jin, S., Dewitz, J., Danielson, P., Granneman, B., Costello, C., Smith, K., & Zhu, Z. (2023).  
 794 National Land Cover Database 2019: A New Strategy for Creating Clean Leaf-On and  
 795 Leaf-Off Landsat Composite Images. *Journal of Remote Sensing*, 3, 0022.  
 796 <https://doi.org/10.34133/remotesensing.0022>
- 797 Ketabchy, M. (2018). *Thermal Evaluation of an Urbanized Watershed using SWMM and*  
 798 *MINUHET: A Case Study of Stroubles Creek Watershed, Blacksburg, VA* [Thesis,  
 799 Virginia Tech]. <https://vtechworks.lib.vt.edu/handle/10919/81977>
- 800 Kofidou, M., & Gemitzi, A. (2023). Assimilating Soil Moisture Information to Improve the  
 801 Performance of SWAT Hydrological Model. *Hydrology*, 10(8), 8.  
 802 <https://doi.org/10.3390/hydrology10080176>
- 803 Krause, P., Boyle, D. P., & Bäse, F. (2005). Comparison of different efficiency criteria for  
 804 hydrological model assessment. *Advances in Geosciences*, 5, 89–97. Proceedings of the  
 805 8th Workshop for Large Scale Hydrological Modelling - Oppurg 2004 - 8th workshop  
 806 for Large-scale hydrological modelling, Oppurg, Germany, 11&ndash;13 November  
 807 2004. <https://doi.org/10.5194/adgeo-5-89-2005>
- 808 Kumar, S., & Merwade, V. (2009). Impact of Watershed Subdivision and Soil Data Resolution  
 809 on SWAT Model Calibration and Parameter Uncertainty. *JAWRA Journal of the*  
 810 *American Water Resources Association*, 45(5), 1179–1196.  
 811 <https://doi.org/10.1111/j.1752-1688.2009.00353.x>



- 812 Kundu, D., Vervoort, R. W., & van Ogtrop, F. F. (2017). The value of remotely sensed surface  
 813 soil moisture for model calibration using SWAT. *Hydrological Processes*, 31(15),  
 814 2764–2780. <https://doi.org/10.1002/hyp.11219>
- 815 López López, P., Sutanudjaja, E. H., Schellekens, J., Sterk, G., & Bierkens, M. F. P. (2017).  
 816 Calibration of a large-scale hydrological model using satellite-based soil moisture and  
 817 evapotranspiration products. *Hydrology and Earth System Sciences*, 21(6), 3125–3144.  
 818 <https://doi.org/10.5194/hess-21-3125-2017>
- 819 Lyon, S. W., Walter, M. T., Gérard-Marchant, P., & Steenhuis, T. S. (2004). Using a  
 820 topographic index to distribute variable source area runoff predicted with the SCS  
 821 curve-number equation. *Hydrological Processes*, 18(15), 2757–2771.  
 822 <https://doi.org/10.1002/hyp.1494>
- 823 Mascaro, G., Vivoni, E. R., & Deidda, R. (2011). Soil moisture downscaling across climate  
 824 regions and its emergent properties. *Journal of Geophysical Research: Atmospheres*,  
 825 116(D22). <https://doi.org/10.1029/2011JD016231>
- 826 Mei, Y., Mai, J., Do, H. X., Gronewold, A., Reeves, H., Eberts, S., Niswonger, R., Regan, R.  
 827 S., & Hunt, R. J. (2023). Can Hydrological Models Benefit From Using Global Soil  
 828 Moisture, Evapotranspiration, and Runoff Products as Calibration Targets? *Water*  
 829 *Resources Research*, 59(2), e2022WR032064. <https://doi.org/10.1029/2022WR032064>
- 830 Moore, C., & Doherty, J. (2005). Role of the calibration process in reducing model predictive  
 831 error. *Water Resources Research*, 41(5). <https://doi.org/10.1029/2004WR003501>



- 832 Moriasi, D. N., Arnold, J. G., Van Liew, M. W., Bingner, R. L., Harmel, R. D., & Veith, T. L.  
 833 (2007). Model evaluation guidelines for systematic quantification of accuracy in  
 834 watershed simulations. *Transactions of the ASABE*, 50(3), 885–900.
- 835 Mullen, K. M., Ardia, D., Gil, D. L., Windover, D., & Cline, J. (2011). DEoptim: An R Package  
 836 for Global Optimization by Differential Evolution. *Journal of Statistical Software*, 40,  
 837 1–26. <https://doi.org/10.18637/jss.v040.i06>
- 838 Nanda, A., Jalilvand, E., Das, N. N., Bindlish, R., & Andreadis, K. (2023). *Optimizing*  
 839 *Hydrologic Model Soil Physical Properties with Smap Soil Moisture: A Pathway for*  
 840 *Skillful Assessment of Streamflow and Drought*. <https://doi.org/10.2139/ssrn.4635449>
- 841 Nash, J. E., & Sutcliffe, J. V. (1970). River flow forecasting through conceptual models part I  
 842 — A discussion of principles. *Journal of Hydrology*, 10(3), 282–290.  
 843 [https://doi.org/10.1016/0022-1694\(70\)90255-6](https://doi.org/10.1016/0022-1694(70)90255-6)
- 844 Nathan, R. J., & McMahon, T. A. (1990). Evaluation of automated techniques for base flow  
 845 and recession analyses. *Water Resources Research*, 26(7), 1465–1473.  
 846 <https://doi.org/10.1029/WR026i007p01465>
- 847 Nayeb Yazdi, M., Ketabchy, M., Sample, D. J., Scott, D., & Liao, H. (2019). An evaluation of  
 848 HSPF and SWMM for simulating streamflow regimes in an urban watershed.  
 849 *Environmental Modelling & Software*, 118, 211–225.  
 850 <https://doi.org/10.1016/j.envsoft.2019.05.008>
- 851 Neitsch, S. L., Arnold, J. G., Kiniry, J. R., & Williams, J. R. (2009). *Soil and water assessment*  
 852 *tool theoretical documentation*. version 2009.



- 853 O'Neill, P. E., Chan, S., Njoku, E. G., Jackson, T., Bindlish, R., & Chaubell, J. (2018). SMAP  
 854 L3 radiometer global daily 36 km EASE-grid soil moisture, Version 5. *Natl. Snow Ice*  
 855 *Data Cent*, 1–82.
- 856 O'Neill, P. E., Chan, S., Njoku, E. G., Jackson, T., Bindlish, R., Chaubell, J., & Colliander, A.  
 857 (2023). SMAP Enhanced L3 Radiometer Global and Polar Grid Daily 9 km EASE-Grid  
 858 Soil Moisture. *Boulder, Colorado, USA: NASA National Snow and Ice Data Center*  
 859 *Distributed Active Archive Center*.
- 860 Parece, T., Dibetitto, S., Sprague, T., & Younos, T. (2010). *The Stroubles Creek Watershed:*  
 861 *History of Development and Chronicles of Research*.
- 862 Patil, A., & Ramsankaran, R. (2017). Improving streamflow simulations and forecasting  
 863 performance of SWAT model by assimilating remotely sensed soil moisture  
 864 observations. *Journal of Hydrology*, 555, 683–696.  
 865 <https://doi.org/10.1016/j.jhydrol.2017.10.058>
- 866 Pechlivanidis, I. G., Jackson, B. M., McIntyre, N. R., & Wheeler, H. S. (2011). Catchment  
 867 scale hydrological modelling: A review of model types, calibration approaches and  
 868 uncertainty analysis methods in the context of recent developments in technology and  
 869 applications. *Global Nest Journal*, 13(3), 193–214.
- 870 Peng, Y., Yang, Z., Zhang, Z., & Huang, J. (2024). A Machine Learning-Based High-  
 871 Resolution Soil Moisture Mapping and Spatial–Temporal Analysis: The mlhrsm  
 872 Package. *Agronomy*, 14(3), 3. <https://doi.org/10.3390/agronomy14030421>



- 873 Rajib, M. A., & Merwade, V. (2016). Improving soil moisture accounting and streamflow  
 874 prediction in SWAT by incorporating a modified time-dependent Curve Number  
 875 method. *Hydrological Processes*, 30(4), 603–624. <https://doi.org/10.1002/hyp.10639>
- 876 Rajib, M. A., Merwade, V., & Yu, Z. (2016). Multi-objective calibration of a hydrologic model  
 877 using spatially distributed remotely sensed/in-situ soil moisture. *Journal of Hydrology*,  
 878 536, 192–207. <https://doi.org/10.1016/j.jhydrol.2016.02.037>
- 879 Sanford, W. E., Nelms, D. L., Pope, J. P., & Selnick, D. L. (2012). Quantifying components of  
 880 the hydrologic cycle in Virginia using chemical hydrograph separation and multiple  
 881 regression analysis. In *Scientific Investigations Report* (2011–5198). U.S. Geological  
 882 Survey. <https://doi.org/10.3133/sir20115198>
- 883 Silvestro, F., Gabellani, S., Rudari, R., Delogu, F., Laiolo, P., & Boni, G. (2015). Uncertainty  
 884 reduction and parameter estimation of a distributed hydrological model with ground  
 885 and remote-sensing data. *Hydrology and Earth System Sciences*, 19(4), 1727–1751.  
 886 <https://doi.org/10.5194/hess-19-1727-2015>
- 887 Sun, L. (2016). *Streamflow and Soil Moisture Assimilation in the SWAT model Using the*  
 888 *Extended Kalman Filter*. <https://doi.org/10.20381/RUOR-4934>
- 889 Thilakarathne, M., Sridhar, V., & Karthikeyan, R. (2018). Spatially explicit pollutant load-  
 890 integrated in-stream *E. coli* concentration modeling in a mixed land-use catchment.  
 891 *Water Research*, 144, 87–103. <https://doi.org/10.1016/j.watres.2018.07.021>
- 892 Vereecken, H., Huisman, J. A., Hendricks Franssen, H. J., Brüggemann, N., Bogaen, H. R.,  
 893 Kollet, S., Javaux, M., van der Kruk, J., & Vanderborght, J. (2015). Soil hydrology:



894           Recent methodological advances, challenges, and perspectives. *Water Resources*  
 895           *Research*, 51(4), 2616–2633. <https://doi.org/10.1002/2014WR016852>

896   Wagner, W., Blöschl, G., Pampaloni, P., Calvet, J.-C., Bizzarri, B., Wigneron, J.-P., & Kerr,  
 897           Y. (2007). Operational readiness of microwave remote sensing of soil moisture for  
 898           hydrologic applications. *Hydrology Research*, 38(1), 1–20.

899   Wagner, W., Lemoine, G., & Rott, H. (1999). A Method for Estimating Soil Moisture from  
 900           ERS Scatterometer and Soil Data. *Remote Sensing of Environment*, 70(2), 191–207.  
 901           [https://doi.org/10.1016/S0034-4257\(99\)00036-X](https://doi.org/10.1016/S0034-4257(99)00036-X)

902   Wakigari, S. A., & Leconte, R. (2023). Exploring the utility of the downscaled SMAP soil  
 903           moisture products in improving streamflow simulation. *Journal of Hydrology:*  
 904           *Regional Studies*, 47, 101380. <https://doi.org/10.1016/j.ejrh.2023.101380>

905   Zeileis, A., Grothendieck, G., Ryan, J. A., Ulrich, J. M., & Andrews, F. (2025). *zoo: S3*  
 906           *Infrastructure for Regular and Irregular Time Series (Z's Ordered Observations)*  
 907           (Version 1.8-14). <https://cran.r-project.org/web/packages/zoo/index.html>

908  
 909  
 910  
 911  
 912  
 913